SEISMIC CAPACITY TESTING OF A THIN WALL 500 TON CYLINDRICAL TANK

Heki SHIBATA(I)

Hiroshi AKIYAMA(II)

This paper was presented at MITI-NRC SIE Meeting in Palo Alto, Calif., U.S.A. in July, 1984. Because of limited circulation, the authors try to present here again with minor modifications.

ABSTRACT

This paper deals with the test project which was done as a part of Seismic Safety Project for High-pressure Gas Facility. For newly building components, like a tower-type vessel (column) and a liquified gass storage in various kind of plants, the MITI Code was established in 1981. Then for exsiting components, the reevaluation of seismic safety margin becomes necessary. Therefore, tests on two types of vessels were done from 1980 to 1983. One was on tower-type vessels and the other one on a thin wall, 500 ton cylindrical tank.

The principal purpose of this experimental work is to clarify the realistic behaviors and the ultimate resistant capacity of liquid-filled cylindrical tanks subjected to destructive earthquake motions. The tank for test was a scale model of a proto-type LNG-tank which had a shallow spherical roof and was anchored by straps at the lower side wall. The dimension of the model was 10 mϕ × 6.9 mH and thickness of wall: 3.2 mm, thickness of annulus ring: 2.2 mm, thickness of bottom plate: 2.0 mm. The tank filled with water, approximately 500 ton, was subjected to the horizontal and vertical input motions of the enlarged Taft earthquake record. The final endurance test was made under the input acceleration of 0.7G of horizontal and 0.5 vertical. As a result, the elephant foot bulging was observed on the circumference, over 40%, of the lower wall.

INTRODUCTION

Recently we developed the aseismic design code for high pressure gas facilities for improving their earthquake resistant capacity. Some damages of such facilities have been observed since Niigata earthquake-1964 in Japan. One of the problems which we have not solved is the buckling-type damage appeared on skirts of tower-type vessels or columns, and also thin wall cylindrical vessels. The examples of failures of thin wall cylindrical vessels are mainly found in those of oil storages, and fortunately no damage of liquefied gas storages has been found up to now.

In this article, the authors will discuss the following items:

i) The new code system for aseismic design of high pressure gas facilities.

I) Professor, Ph.D.
Institute of Industrial Science, University of Tokyo
II) Associate Professor, Ph.D.
Engineering Research Institute, University of Tokyo

ii) The shaking test of tower type vessels purposed to obtain their reviewing criteria for their earthquake resistant capacity.

iii) The shaking test of a thin wall 500 ton storage tank to clarify its failure mechanism and earthquake resistant capacity.

Through these testings, so called " elephant foot buckling " does not appear by one impulsive load generally, and it grows by repeating load caused by earthquake motions. Therefore, this phenomenon might be called as " elephant foot type bulging " rather than buckling.

NEW REGULATORY SYSTEM FOR ASEISMIC DESIGN AND TESTING ON SHAKING TABLE

1) DEVELOPING A NEW REGULATORY SYSTEM

Since 1973, we have been engaging to develop a new regulatory system for aseismic design of high pressure gas facilities, which are deeply related to petro-chemical industry and oil refinary. The final draft[1] came out in 1980. The fundamental principle of the design procedure of earthquake resistant structures, such as tower (column), vessel, equipment and other components was similar to that for nuclear facilities. The development of that for nuclear facilities started in 1958[2], and had been going towards an application of modern dynamic response analysis. In 1973, Kanagawa-pref. introduced this principal design philosophy to the field of high pressure gas facilities[3].

The draft for the new code in 1980 was stayed on the same line to Kanagawa-prefecture's one. And it was reorganized as the MITI (Ministry of International Trade and Industry)-notice #515[4], and was issued in October 1981. At that time, there were several problems for issuing this notice.

One of them was the use of an elasto-plastic energy theory for the design. The application of the plastic energy theory to a spherical liquefied gas storage tank was involved in the draft[1], but it was deleted in the notice[4] of 1981. Another problem was how to treat existing facilities. It was decided that the new notice did not apply to existing ones. However, a destructive earthquake has been expected in Tokai and the Southern Kwanto areas, and it has been the subject how we guarantee their earthquake resistant capacity.

Then we, KHK, Institution for Safety of High Pressure Gas Engineering, organized a committee for the reevaluation program including its guideline, and Professor Inoue took the chair of the committee. They decided to use the simple pseudo-elastic design criteria, for example, the allowable stress of anchor bolts of a tower-type vessel is its ultimated strength S_u. It is more than that for the Faulted Condition of ASME, Boiler and Pressure Vessel Code Section III; or Plant Condition IV of the MITI-notice #505[5]. The principal concept of this pseudo-elastic design came from a plastic capacity design, but it was too simplify to guarantee their capacity. And also there were many uncertainties on the behavior of a tower type vessel and a thin wall cylindrical storage tank for liquefied gas under destructive earthquake conditions.

2) THE CODE SYSTEM

The MITI-notice #515 is supported by the concept which was defined by the order of the Minister of International Trade and Industry as follow: The procedure of aseismic design of high pressure gas facilities specified

in the notice may be replaced by the procedure which is approved to be equal to the procedure in the notice by the Minister. This order opens the new way to use specific computer program for the design analysis. Those programs are not equal to the expression of algorithm specified in the notice. The analysis and design procedure may be different to those in the notice. The result of design analysis by using such a computer code should give at least the equivalent capacity of earthquake resistance to the structure as specified in the notice. The MITI provides a series of the computer codes "SEISMIT". Two codes SEISMIT-TW for a tower-type vessel or column and SEISMIT-SP for a spherical liquefied gas storage are under the operation. One for a horizontal cylindrical vessel, SEISMIT-HV is on the final stage of preparation. One for a supporting structure, SEISMIT-ST is under preparation. Those for a flat bottom cylindrical vessel and a piping system are pending at this moment. Especially, the standard aseismic design procedure of piping systems has been discussed, but still there are many difficulties to cover those from nuclear pipings to barried pipings.

Any engineering organization may submit their own computer program for aseismic design of such structures and equipment related to high pressure gas facilities to the Minister to obtain his approval to be equal computation ability to the notice.

PURPOSE OF TESTINGS

Two tests had been done for last three years as the project of MITI in relation to the reevaluation project on the earthquake resistant capacity of existing high-pressure gas facilities. As described in the previous chapter, the behaviors of a tower-type vessel and a thin cylindrical tank had not been clear, and their failure mechanisms had to be knwon by the testing. Bulgings of a thin cylindrical vessel, which has been called as an elephant foot buckling since San Fernando earthquake-1971, were sometimes observed, but it is clear that the bulgings observed at San Fernando earthquake and Concon earthquake-1965 (Chile, $M = 7\frac{1}{4}$) are different from bucklings with sharp corner observed at Livermore earthquake-1980 (California, $M = 5.5$), San Juan earthquake-1977 (Argentina, $M = 7.0$). Professor Clough and Dr. Niwa[6], EERC, University of California, Richmond made clear this through the testing of the wine tank which was the same size that was damaged by Livermore earthquake. The film of their testing clearly showed that its buckling type deformation of thin shell occured by a single impulsive loading by horizontal excitation.

The mechanism of the elephant foot type deformation was not clear to the author, but he found the following fact in 1976 in Tomakomai, Hokkaido through the resurvey on damage by Tokachi-oki earthquake-1968. The author visited one oil storage station in Tomakomai to resurvey on damage of cylindrical oil storage tanks. He met a person who witted that one cylindrical tank, approximately 1000 ton, was up-lifted in some ten centi-meters. No damage on the tank was found, and still they were using it, when the author was. He examined it and observed that it was slightly deformed like elephant foot type deformation, but it was not like those observed at other earthquakes. He thought that the deformation had been growing gradually, and that it was not like a buckling which was one of unstable phenomena as observed by Professor Clough and Dr. Niwa.

Through the discussion with the members at the Committee of the testing project, and also with the members of the working group for the testing chaired by Akiyama, one of the authors, we concluded that the main target of

our testing would be to clarify the mechanism of elephant foot type deformation wich we called "bulging" instead of "buckling" later, both for a tower type vessel and a thin cylindrical tank.

TESTING OF TOWER-TYPE VESSEL[6]

1) OUTLINE AND ITS RESULT

In the first year of the project 1981, we tested a tower-type vessel or column. At first, we planned to test several specimens including one existing tower which had been used in the field. Finally we decided to test five models which were partially substitute by a weight as shown in Pict. 1. The purpose of testing was emphasized to make clear that their strength and energy absorbing capacity at their lower portion. The size of models was 1200 mm in their outer diameter, and their details were different in each specimens to clear the modes of failure or energy absorption by the different details. On the contrary, in the case of the thin cylindrical tank, only one specimen was available for testing by the restriction of the budget and others. Therefore, the specimens were designed so as to fail at their anchor bolts or skirt. As the details of size of five specimens from T-1 to T-5 are shown in Table 1, the thickness of the skirt of each specimen changed from 5.55 mm to 9.25 mm, and the diameter of sixteen anchor bolts of each specimen changed from 30 mm to 48 mm. The weight of its upper part was 50 ton and the height of its center of gravity was 4800 mm, and it gave the overturning moment whose height was assumed to be approximately 20 m. Their foundation was made of the reinforced concrete to give an equivalent supporting condition of the actual tower type vessel or column.

The shaking table for the test was the 500 ton one in National Disaster Prevension Center in Tsukuba Science City. Their vibration characteristics are as shown in Table 2. The number of bolts was reduced into four from sixteen in some testing conditions, especially T-5 and some cases of T-1 and T-4 were tested only four bolts.

By using single axis input of the following three natural earthquake records, Imperial Valley earthquake-1940 NS at El Centro, Kern Country earthquake-1952 EW at Taft and Tokachioki earthquake-1968 NS at Hachinohe, and also sinusoidal waves near to its resonance condition. Key data of the testings are shown in Table 3. Each specimen was tested four to six times except T-5. The last one was tested to reach to its failure state by a single test. If anchor bolts had their full capacity of sixteen, all specimens, that is, T-1 to T-4, were buckled at their skirt. In the case of T-1, it caused by El Centro $\sim$ 941 Gal input, but its resistant capacity was not changed. In the case of T-2, whose anchor was stronger than that of T-1, the buckling phenomenon was observed in the sinusoidal resonance tests, and obviously its resistant capacity was lowered after it buckled, and finally the skirt had a crack along the top of its bending wave by fatigue. Its wave form was not formed clearly by a single pulsive loading, and was gradually forming its buckling-like shape. The authors will discuss this problem in the following chapter more precisely. In the case of T-3, this phenomenon was observed in sinusoidal resonance test also. Their wave lengths were approximately 150 mm, and they started from the upper corner of compression ring, and this shape was similar to the static buckling test result.

T-4, whose skirt was thicker than those of the previous three specimens, also cause the same type of deformation. The discontinuity of time-strain

curve was observed sharply, but the deformation of the shell was not observed at first. Sometimes, the sound of druming of shell was recognized. If reduced the number of anchor bolts, their yieldings were clearly observed by removing of black rust skin.

After the dynamic testings on the shaking table, a static loading test so as to produce the buckling on their skirts was made by a simple bending test on the beam which consisted from T-1 and T-4 welded together at their bottoms. Through this testing the same type buckling to those observed in the dynamic tests was obtained. The wave length of deformation was again 150 mm, and its depth was approximately 10 mm, and its load-deformation curve is shown in Fig. 1.

2) EVALUATION OF TESTING RESULTS

Based on these testing data, some values of their critical loads were estimated as shown in Table 4. This evaluation were made by Akiyama, one of the authors, and the followings are the brief explanations of testing results.

i) Strength of the foundation concrete

No damage was observed on any part of the foundations.

ii) Strength of the anchor bolts

They were yielded in some tests. The safety factor S_b obtained by the following ratio;

$$S_b = Q_{max,\ b,\ m} \ / \ Q_{y,b} \tag{1}$$

was in between 1.0 and 1.31, where $Q_{max,\ b,\ m}$ is the maximum horizontal force recorded at the testings, and $Q_{y,b}$ is the strength of anchor bolts defined by the yielding strength of their shanks. These values were observed in the case in Table 5, and indicated "B" in Table 1.

iii) Critical limit of buckling at the skirt

The cases indicated "S" in Table 1 were buckled at their skirt. The criteria of buckling limit for the design are various according to the fields related to. For the high pressure gas facilities, the following criteria has been used

$$\sigma_{cr,s} = \frac{0.6\ Et}{\left(1 + 0.004\ \frac{E}{\sigma_y} \right) D} \tag{2}$$

where D is the diameter of the skirt and other notations are common ones. This equations is the modification of Donnel's equation

$$\sigma_{cr} = \frac{E\left(\frac{0.6t}{R} - \frac{R}{10^7 t} \right)}{\left(1 + 0.004\ \frac{E}{\sigma_y} \right)} \tag{3}$$

where R is the radius of the skirt. This equation is obtained by eliminating the term of $R/10^7 t$, and introducing the safety factor 2.

The critical horizontal force Q_{cr} is defined from the critical overturning moment M_{cr} which obtained by the following equation,

$$M_{cr} = \sigma_{cr} \left(1 - \alpha\ \frac{\sigma_c}{\sigma_{cr}} \right) Z \tag{4}$$

where σ_c is the average compressive stress by axial force, Z is the coefficient of cross section of the over all skirt cross section. The coefficient α is usually taken larger than unity, here Akiyama, one of the authors, assumed as a unity. Critical limits in Tables 3 and 4 were the values in Fig. 2. The value for T-1, T-2 and T-3, that is, the thinner ones is σ_{cr} = 2.64 ton/cm^2, and this value was evaluated from the result of the static bending test of a beam consisting of T-1 and T-4 which were welded together as mentioned-above. Through this testing, Q_{max} was recorded as 38.1 ton, and σ_{cr} was obtained by this testing result. The value for T-4 and T-5, that is, the thicker skirt one is 2.47 ton/cm^2. This value was obtained by the dynamic test of T-4. By the sinusoidal resonant test, its skirt was partially buckled. Then this σ_{cr} was obtained from M_{cr} by Eq. (4). The relation of those two values to the criteria for high-pressure gas facilities is shown in Fig. 1. To that for nuclear containment vessel is different from the relation in Fig. 1. Those have a certain margin to the criteria for high-pressure gas facilities.

In Table 4 some relation of Q_{max} obtained by the static test to the experimental results are shown. In the cases of T-1-3 and T-4-4, their anchor bolts were failed, therefore the factors were less than unity. In the case of T-3, all results exceeded Q_{cr} , and $Q_{cr,y}$ was also compared to those, where $Q_{cr,y}$ is the loading for resisting force by a simple compressive yielding. It should be notice that the testing results of T-3 were stronger than the value of resistance obtained by this mode of failure. This may be caused by the effect of its strengthening ring at the bottom of the skirt.

ENERGY ABSORPTION CAPACITY OF TOWER-TYPE VESSEL

Earthquake motions bring the energy E to the system, and this energy is absorbed by plastic deformations of anchor bolts and skirt. The safety coefficient σ is defined as follows:

$$\sigma = \frac{E}{E_p + E_e} \tag{5}$$

where E_p is the estimated total energy absorbed by plastic deformations when it reaches to the critical load, and E_e is the maximum dynamic energy in the system when the system reaches to yielding level. In Table 6, the values of Eq. (5) are shown for each testing. In the cases of sinusoidal inputs, this ratio reached to very large value compare to the unity. This means that it absorbed large amount of energy until the low-cycle fatigue crack was observed. In the cases of anchor bolts failure, the value σ is approximately two. This means that other parts might absorb the energy as well as anchor bolts.

Through these testings in the initial phase of so-called elephant foot buckling, no deformation was observed, and the deformation gradually increased by repeating bending load to the shape of an elephant foot bulging and finally reached to cause a crack by the low-cycle fatigue effect as previously mentioned. However, total energy input to reach this state may be far larger than the energy to cause the first buckling in the

case of tower-type vessel. This ratio may be a function of its dimension and input wave forms. Some values, whose failure modes were clear, are shown in Table 6.

From such a total absorption capacity, an equivalent velocity or acceleration of ground motions can be defined by assuming the parameters of a structure like its eigen-period and so on. If the ratio η is defined as follow:

$$\eta = E_p / E_e \tag{6}$$

then

$$\frac{\alpha}{\alpha_0} \text{ or } \frac{V}{V_0} = \frac{1}{\sqrt{1 + \beta\eta}} \tag{7}$$

The value α_0 or V_0 is the acceleration or velocity for producing elastic limit response to the structure. The value β may be 1.0 to 1.5. Through the result shown in Table 6, the authors judged that β might be 1.5.

TEST OF 500 TON THIN WALL CYLINDRICAL STORAGE TANK

1) OUTLINE AND ITS RESULT

In 1982 and '83, the second phase of the project had been made. The seismic resistant capacity of a thin wall cylindrical storage tank was investigated. The main purpose of the project was to know the behavior of its thin side wall in the similar viewpoint to that of the tower type vessel discussed in the previous chapters.

The original one is an anchored thin wall cylindrical storage tank for liquefied gas storage which is regulated by the law for high pressure gas facility. But the model for testing was designed to have appropriate dimension to a shaking table proposed for the use.

The shaking table, Tadotsu Engineering Laboratory, NUclear Power Engineering Testing Center, was proposed for this test. To meet the size and the capacity of this shaking table, the test specimen had a 10 m diameter and a 6.9 m height, and its capacity was approximately 500 m^3. Its details were similated to that of a 50000 m^3 class vessel. The thickness of the side wall was 3.2 mm and that of the bottom plate was 2.0 mm and 2.3 mm for annular part. The schematic drawing is shown in Fig. 3. These dimensions were extremely thin compared to its whole dimension. It set on a pearlite concrete foundation as most of real size Liquefied National Gas storages are. To prevent the trouble of leaked water, the outer containment was provided. This, 13000 mm diameter steel vessel was sufficiently stiffened on its cylindrical wall. The thickness of pearlite concrete was 300 mm, and sat on H-beam foundation grid, whose pitch was 1050 mm. This grid was tightend to the table with 72 anchor bolts. The anchor straps were welded at every 10 degree points on its circumference along the 600 mm height of the wall, and their lower ends were welded to the grid. Their cross-section was 60 mm × 4.5 mm. The material of most of the inner vessel was a mild carbon steel, SS-41. The total weight was 103 ton, and it was fabricated in the out door near by the table, brought in through the access road, and finally settled by two overhead cranes on the table. So, there were some residual strain of the grid and anchor straps were observed after all anchor bolts were tightened. Picts. 2 and 3 are shown its appearance.

2) INSTRUMENTATION AND DETAILS OF TESTING

Fifty acceleration pick-ups, forty displacement sensors, ninety-four strain gauges, thirteen pressure gauges, and three wave hight pick-ups were installed. Also hydraulic pressure of actuators were recorded to decide the reaction forces from the specimen. This data gave various information through the data analysis procedure. One computer was used for this purpose in addition to the original system.

The lay-out of these instruments was made to obtain the following four informations:

i) Excitation and reaction of the table.
ii) Acceleration distribution and inertia distribution.
iii) Water pressure distribution.
iv) Strain distribution.

All those information were converted into load level time histories and peak values, and compared to each others. It was expected that the response of the shell should be parallel to direction of the horizontal exciting force. However, it was not exactly parallel to the excitation direction, and the arrangements of instrumentation were made by the assumption above. The discrepancy of the direction between excitation and response was approximately 25°, and it was estimated coming from the distorsion of the grid. Therefore, some data, especially, strain ones were not sufficient.

Testings were done as shown in Table 7(a) and (b) for full level water (550 ton), and seven inputs for 60% level water. Most of the testings in full level were intending to observe its impulsive type response. Test #1 (FSH) and #2 (FSV) were the sinusoidal sweep tests to obtain its vibration characteristics. Test #3 (FHAC-1/8), and #4 (FCOS-1) and #9 (FCOS-2) were done mainly to observe its sloshing response. All others from #5 to #12 were made by using Kern County earthquake-1952 record in Taft.

Tokachi-oki earthquake-1968 in Hachinohe contains longer period components compare to earthquake records in the U.S.. The Taft records using for these testings were shortened in $\frac{1}{\sqrt{5}}$, because its scale factor in dimension was assumed to be 1/5. The fragility tests from #8 to #12 except #9 were based on #8 (FTFS-1.0), by the full hight modified Taft earthquake record, and increased as 1.5 times, 2.25 times and 3 times. The increase of input levels were made according to the result of the previous test one. Tehrefore, for the test #12 (FTFS-3.0), the level of vertical component was kept to equal to the previous test #11 (FTFS-2.25), that is, the horizontal component was 3 times, and the vertical component was suppressed to 2.25 times. On the table, the notation "IC" means the wave form compensations were made based on its numerical model only before shaking. And "RC-n" means that the compensations were made n times based on the reconstructed numerical model by the previous test. For the fragility tests, the repetition was not made to avoid the excess effect by low-cycle fatigue at the welded joint. The crack at the corner of the bottom plate and the side wall was expected, but it was rather difficult whether or not to estimate the jet of 550 ton water was completely safe to the table.

3) TEST RESULT AND ITS ANALYSIS

At first, the impulsive type responses to horizontal and vertical directions were studied. Compared to the testing result, the result of analysis by using ordinary FEM method for a coupled system was examined.

The effect of its roof portion was assumed to be an additional mass, and no consideration on their stiffness. The vibration characteristics are shown in Table 8. Some discrepancies were found by measuring devices, and the natural frequencies obtained by testing were slightly lower than the results of analyses made by various ways.

The response curves of the acceleration on the shaking table in the various level are shown in Fig. 4. And the time history of the energy inputs are shown in Figs. 5(a) and (b). These were obtained by the data on the reaction force of the table observed by the hydraulic pressure of the actuators. In Fig. 6, the same type of the curves, obtained by the water pressure responses on the side wall, is shown. Both in Figs. 5(a) and 6 shows a good coincidence. The comparison of various resultant forces was also made, and they show good agreement to each others.

Some results of its responses to various inputs at the full level water test are shown in Table 9. The ratio D_s of the effective response A_f, this is defined by the reaction force devided by its mass to the response A_E obtained by an elastic single mass-spring model in Table 9 is considered to be an index of its plastic behavior. It should be noticed that A_E was obtained by the total response energies for both exciting directions, whose values were evaluated from the time histories of reaction forces in Figs. 6 and 5(b). The value D_s are around 0.5, but it can be lower than the value expected based on input acceleration level in some cases.

4) STRAIN AND ELEPHANT FOOT TYPE DEFORMATION

The deformation was assumed to be a shape as with up-lifting. In this case, a buckling or bulging can be expected at the compression side, and a failure of bottom plate near its welded joint can be expected at the tension side.

The mode shape expressed by the pressure distribution shown in Figs. 7(a) and (b) with some computation results. The observed values were not symmetrical. However, the strain distribution was almost axi-symmetrical, but slightly deviated as shown in Fig. 10. The numerical result based on rigid wall assumption by using the Housner's method[7] appeared in TID Report is obviously lower than others. However, in the case of 60% level, the observed values were almost equal to the result by the Housner's method. One of the examples of the two dimensional response of dynamic pressure variation is shown in Fig. 8. The solid-line shows the result of numerical calculation using SRSS scheme P_{cal}, and the dotted-line shows the result P_A obtained by the effective horizotal acceleration A_f.

The bending stress or strain in the lower portion of the side wall is the most significant result in this project. The ratio of observed values $\sigma_{b,m}$ to those σ_b obtained by the assumption of the fixed end shows the variation from 3 to 17.

Akiyama, one of the authors, recommended the factor "4" to estimate $\sigma_{b,m}$ for design practice from these results. However, in the case of this testing, the input accelerations, or the seismic coefficients were relatively high compared to the level of yielding of its shell, and also the tests were repeated after partial buckling occurence. One of examples of the coefficient γ for estimating $\sigma_{b,m}$ calculated for a 75000 kl storage with

anchor straps by Dr. Asai is shown in Fig. 9[8]. This result clearly shows that the coefficient γ is approximately 1.1 to 1.2, and did not go up to 4 after the side wall reached to yielding state. This value is a function of the spring constant K_v at the edge of the bottom. If the spring constant is assumed to be very high as $K_v = 4 \times 10^4$ kg/cm/cm, it is around 2, and still far lower than 4 of the testing result. The reason it reached to such a high value has not been clear, however, the progressive plastic deformation may occure by repeating uplists. And it should be noticed that this index is also a function of the state of anchor straps. Without anchor strap, this index may reach to 4, even under a very low level input condition.

In this paper, those values like $\sigma_{b,m}$ are expressed by nominal stress, and they should be read in a strain value. The figures like Fig. 10 shows a nominal resultant surface stress, but the actual value observed is a strain. This figure (Fig. 10) shows the nominal resultant surface stress of the wall near to the bottom observed at the fragility tests, Test #8. The surface stress σ_s exceeded the yielding stress σ_y in the case of Test #12. It should be noticed this value also exceeded the yielding stress near to the welded joint. Such over-stress (strain) caused the elephant foot bulging. The development of bulging regions is shown in Fig. 11. Actually, it started at the short period resonance test (FCHH-1.0) which was done as a part of Test #1 to make sure the resonance point. It was unexpected phenomenon, and the bulging had been developed as shown in Fig. 11, and finally reached to the state shown in Fig. 12, where l is the depth of bulging and h is the height of hoop. The values observed at the lower portion of the wall are shown in Table 10. The value μ is defined as follow:

$$\mu = \frac{2}{3} \frac{\sigma_{b,m} / \sigma_{y,v}}{1 - \left(\frac{\sigma_{a,m}}{\sigma_{y,v}} \right)^2} \tag{8}$$

where, $\sigma_{y,v}$ is the vertical yielding stress under bi-axial stress condition. If this μ will exceed the unity, the bulging is starting to deform.

Its anchor straps were loosened by such bulging of the shell. When the vessel was up-lifted, the loosen straps tautened and clapped. Therefore, the use of high tensile stress steel for anchor strap or bolt should be carefully examined in the view point of its brittle fracture. A typical example of a loosened strap is shown in Pict. 4, and the state of bulging is shown in Pict. 5.

The amount of uplifting is shown in Fig. 14 as δ_v. This value is almost proportional to the effective input acceleration A_f defined in the previous section, and it reached to over 8 mm, and is considered to be significantly large for the tank of this size. And it should be noticed that it caused the sway motions δ_h of the same order as shown in Fig. 14 as well as the elastic response of δ_t in Fig. 13.

5) HYDRAULIC EFFECT OF SLOSHING PHENOMENON AND ITS EFFECT ON NUCKLE PART

In some cases of the past earthquakes, such as Niigata earthquake-1964, Alaska earthquake-1964, San Fernando earthquake-1971, Nihonkai-chubu earthquake-1983, the sloshing phenomena were observed. If they respond to

longer period of ground motions, wave head will hit the nuckle part or corner ring part of the vessel, and cause impulsive hydraulic pressure on the part of the shell. This is significant for its failure as well as the dynamic hydraulic effect on the wall.

This test did not emphasize such phenomena compared to bulging phenomenon. In Table 11, some comparisons of data are shown. Results of several computational methods are compared to those of testings. Even though the result on the impulsive force by wave head shows some good agreement, the pressure effect of a tongue part of the shocked wave shows a large descrepancy. Although several reasons can be mentioned, but the exact reason has not known from this testing. The smaller size and more precise testings may be necessary to clarify such problems.

The dynamic hydraulic pressure variations at the wall coincided with the numerical results by Housner's rigid wall method in general. The dynamic mass ratio m_s / m_l calculated from the test result is shown in Fig. 15. From this value, the effective mass m_f for its acceleration type response is easily obtained as follows:

$$m_f = m_l - m_s \tag{9}$$

where m_l is the total mass of liquid. The effective mass for vertical excitation is equal to the total mass in the most of cases.

CONCLUDING REMARKS AND ACKNOWLEDGEMENT

Through these testings, the bulging phenomenon which is usually called an " elephant foot buckling " can be clarified. This type of deformation starts by exceeding the buckling criteria, however, deformation, that is a bulging shape, is gradually forming by repeating force. If their wall is thin, and if there is some initial deformation caused by internal pressure and/or other causes, they may start without a buckling phenomenon. Akiyama, one of the authors, is going to discuss this subject in the near future.

This process can be estimated by elasto-plastic response approach with input energy. The catastrophic failure of its side wall or bottom plate may be seldom, and can be estimated by low-cycle fatigue analysis on its local portion. The accidents observed in several past earthquakes had some reasons; for example, the decrease of the plate thickness by corrosion, the poor welding, the effect of a connected pipe, and so on.

The more precise testings on low-cycle fatigue and energy absorbing capacity on local portion by full size but local portion specimens are necessary to establish the design criteria of elasto-plastic design. And also by using smaller size models, the testings on the up-lifting response may be necessary to know the exact behavior under destructive earthquake conditions.

Recently, February 1985, one of the authors received a letter from Mr. M. Watanabe, an engineer of the oil refinary department of Nippon Kōgyo Co.. He mentioned a paper[9] written by Dr. M. Yamada. In the paper, the elephant foot bulging is discussed in relation to other types of buckling of cylindrical shell. It suggests that the types of bucklings of the towers and the cylindrical shell discussed in this article may be different to each other in the view point of the initiation of their deformation. The authors will discuss this point in the near future.

These testings and the analyses were done by the working group, then they stayed at Tadotsu more than three weeks in the Summer of 1983, and

they completed this elaborate works. The testing on tower type vessels was done also in the same situation. And the detailed results discussed in this article were analized by Akiyama and the members of the working group.

Through all processes of planning, designing, manufacturing and testing, the cooperations of the staffs of Institution for Safety of High Pressure Gas Engineering have been great. The authors, likes to express their deep gratitude to those related persons.

And also they appreciate having the chance to clarify the mechanism of unknown elephant foot deformation of such structures by the effort of Industrial Location and Environmental Protection Bureau, the Ministry of International Trade and Industry.

Finally they also appreciate the interests on this subject from Professor R.W. Clough, EERC, University of California, Richmond.

REFERENCES [** indicates Japanese written material]

[1] Shibata, H. *trans.*: Draft of Anti-earthquake Design Code for High-pressure Gas Manufacturing Facilities, *Report of ERS* (Inst. of Ind. Sci., Univ. of Tokyo), No.III-5 (July 1981), 30pp.

[2] Shibata, H.: Aseismic Design of Nuclear Power Plants - Developments of These Ten Years, NSJ-Tr161 (Japan Atomic Energy Research Inst.) (Nov. 1970), 27pp.

[3] Kanagawa-pref.: Guideline for Aseismic Design of High-pressure Gas Manufacturing Facilities, (April, 1973), 11pp.**

[4] Ministry of International Trade and Industry: Anti-earthquake Design Code for High-pressure Gas Facilities, The Notice of the Ministry of International Trade and Industry, No.515 (Oct. 1981).**

[5] Ministry of International Trade and Industry: Code for the Detailed Design of Nuclear Power Plant Facilities, The Notice of the Ministry of International Trade and Industry, No.505 (*rev.* Oct. 1980).**

[6] The Seismic Testing Committee, KHK: Earthquake Resistant Test of Tower-type Vessels, *J. of KHK (IHPGE) "Kōatsugas"*, Vol.19, No.10 (Oct. 1982), p.497.**

[7] USAEC (Housner, G.): Dynamic Pressure on Fluid Containers, Chapt. 6, *Nuclear Reactor and Earthquake* TID 7024 (Aug. 1963), p.183.

[8] Asai, O. and others: Axial Compressive Force of Cylindrical Tank Shell Plate with Consideration of Anchor Strectling under Seismic Loading, *J. of HPI*, High Pressure Technology Institute, in printing.**

[9] Yamada, M.: Elephants Foot Bulge of Cylindrical Steel Tank Shells, *J. of HPI*, Vol.18, No.6 (Nov. 1980), p.287.**

Table 1 Size and Characteristics of Tower-type Vessel (Column) Specimen

Code of Specimen	Diameter (mm)	Skirt			Anchor Bolt					C.G. Eff. Hight (mm)	Weight (ton)	Exp. Failure Mode
		Thickness (mm)	σ_y (Kg/mm^2)	σ_u (Kg/mm^2)	Diameter (nominal) (mm)	Number	Effective Cross Section (mm)	σ_y (Kg/mm^2)	σ_u (Kg/mm^2)			
T-1	597	5.55	28.1	38.0	30	16	561	28.1	44.2	472	53.5	S,B
T-2	597	5.55	28.1	38.0	42	16	1121	29.8	48.3	467	53.5	S
T-3	597	5.55	28.1	38.0	48	16	1473	30.0	48.9	462	53.5	S
T-4	596	9.25	32.2	49.9	42	16	1121	29.8	48.3	467	53.6	S,B
T-5	596	9.25	32.2	49.9	48	16	1473	30.0	48.9	462	53.6	S,B

S: Skirt Buckling
B: Anchor Bolt Failure

Table 2 Performance of Tsukuba Shaking Table

I) HYDRO-ELECTRIC SERVO-DRIVING,
II) DISPLACEMENT CONTROL,
III) HORIZONTAL OR VERTICAL SINGLE COMP. EXCITATION,
IV) MAX. CAPACITY, 500 TON IN HORIZONTAL,
V) TABLE SIZE 15 X 15 M AND 12 X 12 M NET,
VI) MAX. VECTOR FORCE 360 TON G,
VII) MAX. ACCELERATION 0.55 G IN FULL LOAD,
VIII) MAX. VELOCITY 37 CM/SEC,
IX) MAX. DISPLACEMENT $\pm$30 MM,
X) FREQUENCY RANGE 0.1 $\sim$ 50 HZ,
XI) CONSTRUCTION WAS COMPLETED IN JUNE 1970,
XII) NATIONAL DISASTER PREVENTION CENTER, SCIENCE AND TECHNOLOGY AGENCY.

Table 8 Comparison of Eigen Frequency and Critical Damping Ratio of Tank

		Eigen Frequency f (Hz)		Damping Ratio ζ [%]	
	Water Level	60%	100%	60%	100%
Horizontal Ex.	By Shell Acc.	9.72	6.37	3.33	2.11
	By Shell Strain	9.64	6.36	3.01	1.79
	By Water Pressure	9.65	6.33	3.01	0.66
	FEM Comp.	12.92	8.70	----	----
	Comp. by Fujita's Method (Ref. 8)	12.89	8.47	----	----
Vertical Ex.	By Shell Acc.	10.26	7.42	1.49	0.64
	By Shell Strain	10.15	7.39	2.41	0.87
	By Water Pressure	10.14	7.37	2.09	0.62
	Comp. by Sakai's Method	13.18	8.70	----	----

Table 3 Some Results of Testing of Tower

Test Number	T-1-1	T-1-3	T-1-4	T-2-1	T-2-3	T-3-1	T-3-5	T-4-1	T-4-4	T-5
Number of Anchor Bolts	16	8	4	16	16	16	16	16	8	4
Input Ground Motion; Type and Peak Acc.' [Gal]	TAFT 390	EL CENTRO 340	EL CENTRO 340	TAFT 100	SINUSOIDAL (2.95Hz)	TAFT 400	TAFT 400	TAFT 400	SINUSOIDAL (1.9 Hz)	SINUSOIDAL (1.5 Hz)
Critical Tensile Force at Anchor Bolt T [ton]										
A) By Anchor Bolt's Yielding	159.4	79.7	39.9	330.2	330.2	434.4	434.4	330.2	165.1	108.6
B) By Iron Bar Yielding Beam	265.3	275.5	259.8	266.3	266.3	474.8	474.8	472.1	472.1	---
C) By Shear Failure of Beam	588.5	588.5	588.5	596.1	596.1	607.1	607.1	597.1	597.1	608.1
Compressive Stress at Skirt σ_c [Kg/mm^2]	2.6	2.6	2.6	2.6	2.6	2.6	2.6	1.55	1.55	1.55
Critical Stress of Skirt σ_{cr} [Kg/mm^2]	26.4	26.4	26.4	26.4	26.4	26.4	26.4	24.7	24.7	24.7
Critical Horizontal Shear Force										
A) By Buckling Q_{cr} [ton]	31.3	31.3	31.3	31.7	31.7	32.0	32.0	51.2	51.2	51.7
B) By Anchor Bolt's Yielding $Q_{cr,b}$ [ton]	39.7	24.4	14.3	75.8	75.8	98.8	98.8	75.7	38.2	28.2
Maximum Horizontal Input Force by Testing $Q_{max,m}$ [ton]	30.6	25.5	18.7	36.9	33.9	39.3	35.7	43.5	44.6	35.7
Maximum Input Energy by Earthquake Motion E [ton-cm]	83.3	98.0	119.1	89.3	2619	142.9	154.8	71.4	726.2	571.4
Maximum Dynamic Energy at Yielding Level E_e [ton-cm]	29.9	22.4	13.3	26.0	26.0	25.3	25.3	48.9	37.8	25.3
Ratio of E to E_p	2.8	4.4	9.0	3.4	100.7	5.6	6.1	1.5	19.2	22.6

Underline on Q_{cr} or $Q_{cr,y}$ is showing the minimum limitation of horizontal shear resistance value.

Table 4 Comparison of Shear Forces; Test and Estimation on Skirt

Test Number	T-1-1	T-1-2	T-1-3	T-2-1	T-2-2	T-2-3	T-2-4
Maximum Horizontal Input Force by Testing $Q_{max,m}$ [ton]	30.6	34.9	25.5	36.9	32.6	33.9	33.3
Critical Horizontal Shear Force							
i) By Buckling Q_{cr} [ton]	31.3[0.98]	31.3[1.12]	31.3[0.81]	31.7[1.16]	31.7[1.03]	31.7[1.07]	31.7[1.05]
ii) By Compressive Yielding of Skirt $Q_{cr,y}$ [ton]	------	------	------	------	------	------	------

	T-3-1	T-3-2	T-3-3	T-3-6	T-4-2	T-4-4	
	39.3	39.9	37.5	37.5	51.2	44.6	
	32.0[1.23]	32.0[1.25]	32.0[1.17]	32.0[1.17]	51.2[1.00]	51.2[0.87]	
	34.3[1.15]	34.3[1.16]	34.3[1.09]	34.3[1.09]	------	------	

i) In [ ], the ratio of testing result to the estimated critical value is shown.
ii) Under-lined tests; see Table 5.

Table 5 Comparison of Shear Force; Test and Estimation on Anchor Bolts

Test Number	T-1-3	T-1-4	T-4-4	T-5
Maximum Horizontal Input Force by Testing $Q_{max,m}$ [ton]	26.5	18.7	44.6	35.7
Critical Horizontal Shear Force by Anchor Bolt's Failure $Q_{y,b}$ [ton]	24.4[1.05]	14.3[1.31]	38.2[1.17]	28.2[1.27]

See the foot note of Table 3.

Table 6 Comparison of Absorbed Energy

Test Number	T-1-1	T-1-2	T-1-3	T-1-4	T-2-1	T-2-2	T-2-3	T-2-4	T-3-1	T-3-2
Input-motion Type and Failure Mode	EQ,OT	EQ,OT	EQ,B	EQ,B	EQ,OT	EQ,QT	SIN,S	SIN,S	EQ,OT	EQ,OT
Maximum Input Energy by Earthquake Motion E [ton-cm]	83.3	50.0	98.0	119.1	89.3	41.7	2619	3571	142.9	166.7
Maximum Dynamic Energy at Yielding Level E_e [ton-cm]	29.9	29.9	22.4	13.3	26.0	26.0	26.0	26.0	25.3	25.3
Total Absorbed Energy by Plastic Deformation E_p [ton-cm]	NE	NE	39.9	39.9	NE	NE	80.8	229.5	NE	NE
Safety Coefficient for Energy Absorption α	2.8	1.7	1.6	2.2	3.4	1.6	24.5	14.0	5.0	6.6

T-3-3	T-3-4	T-3-5	T-3-6	T-4-1	T-4-2	T-4-3	T-4-4	T-5
EQ,OT	EQ,OT	EQ,OT	SIN,S	EQ,OT	SIN,OT	SIN,OT	SIN,B	SIN,B
166.7	154.8	154.8	857.1	71.4	273.6	321.4	726.2	571.4
25.3	25.3	25.3	25.3	48.9	48.9	37.8	37.8	25.3
NE	NE	NE	157.3	NE	NE	NE	257.6	256.3
6.6	6.1	6.1	4.7	1.5	5.6	8.5	2.9	2.2

EQ: Earthquake Motions
B: Bolt Failure
NE: not estimated
S: Skirt Buckling
SIN: Sinusoidal Motions
OT: Elastic or Energy was absorbed at unknown part.

Table 7(a) Full-level Liquid Performance Survey Tests of Thin-wall Tank

Test Number			1	2	3	4	5	6	7
Test Code			FSH	FSU	FHAC-1/8	FCOS-1	FTFV-1/4	FTFH-1/4	FTFS-1.4
Wave Form			SINUSOIDAL SWEEP	SINUSOIDAL SWEEP	HACHINOHE -NS	SINUSOIDAL 3-WAVES	TAFT-UD	TAFT-EW	TAFT-EW -UD
Input Level			16 [Gal]	20 [Gal]	1/8	±25 [mm]	1/4	1/4	1/4
Input Correction			RC-1	IC	IC	IC	RC-1	RC-1	RC-1
Testing Result	Table Acc. [Gal]	Hor.	25.7	---	36.7	13.5	---	45.2	47.7
		Vert.	---	27.6	---	---	24.5	---	25.5
	Resp. Acc. [Gal]	Hor.	130	---	94.9	14.2	---	124	138
		Vert.	---	120	---	---	51.0	---	120
	Resp. Disp. [mm]	Hor.	2.05	---	2.15	2.15	---	3.66	1.83
		Vert.	---	---	---	---	---	---	---
	Resp. Factor	Hor.	5.06	---	2.59	1.51	---	2.74	2.89
		Vert.	---	4.34	---	---	2.08	---	4.71

Table 7(b) Full-level Liquid, Endurance Tests of Thin-wall Tank

Test Number			8	9	10	11	12
Test Code			FTFS-1	FCOS-2	FTFS-1.5	FTFS-2.25	FTFS-3
Wave Form			TAFT-EW -UD	SINUSOIDAL 3-WAVES	TAFT-EW -UD	TAFT-EW -UD	TAFT-EW -UD
Input Level			1	±60 [mm]	1.5	2.25	3/2.25
Input Correction			IC	IC	IC	IC	IC
	Table Acc. [Gal]	Hor.	200	30.1	329	530	742
		Vert.	117	---	193	286	273
Testing Result	Resp. Acc. [Gal]	Hor.	613	27.4	1053	---	---
		Vert.	539	---	986	---	---
	Resp. Disp. [mm]	Hor.	9.26	2.71	15.0	22.0	33.0
		Vert.	---	---	---	---	---
	Resp. Factor	Hor.	3.07	0.91	3.20	---	---
		Vert.	4.61	---	5.11	---	---

Table 9 Comparison of Response and Response Factor

	Test Number	8	10	11	12
	Test Code	FTFS-1	FTFS-1.5	FTFS-2.25	FTFS-3
Horizontal Excitation	Input Acc. A_0 [Gal]	200	329	530	742
	Equipment Input Velocity V_0 [cm/sec]	30.7	49.5	93.3	130.7
	Equivalent Resp. Velocity V_E [cm/sec]	29.8	41.1	61.4	87.0
	Shear Force at Bottom Q_x [ton]	±130	+206 -175	+303 -218	+345 -272
	Effective Resp. Acc. A_f [Gal]	340	539	793	903
	Equivalent Resp. Acc. A_E [Gal]	1029	1294	1715	2437
	Response Factor A_f / A_0	1.70	1.64	1.49	1.22
	D_s -Value A_f / A_E	0.33	0.42	0.46	0.37
Vertical Excitation	Input Acc. A_0 [Gal]	117	193	286	273
	Equivalent Input Velocity V_0 [cm/sec]	17.1	28.2	41.7	39.8
	Equivalent Resp. Velocity V_E [cm/sec]	16.9	27.6	47.4	49.6
	Vertical Reaction Force R_v [ton]	+173 -180	+274 -239	+334 -322	+299 -311
	Effective Resp. Acc. A_f [Gal]	321	488	595	554
	Equivalent Resp. Acc. A_E [Gal]	705	1151	2003	2096
	Response Factor A_f / A_0	2.74	2.53	2.08	2.03
	D_s -Value A_f / A_E	0.46	0.42	0.30	0.26

Table 10 Comparison of Stress Value and Resultant Bending Moment Ratio

Test Number	8	10	11	12
Test Code	FTFS-1	FTFS-1.5	FTFS-2.25	FTFS-3
Hoop Stress σ_r [Kg/mm^2]	14.97	17.23	19.14	19.25
Axial Comp. Stress σ_c [Kg/mm^2]	6.84	8.96	14.12	15.56
Bending Stress σ_b [Kg/mm^2]	11.83	15.67	19.35	19.71
Estimated Yielding Strength of Material $\sigma_{y,e}$ [Kg/mm^2]	19.01	16.83	14.83	14.71
Resultant Bending Moment Ratio M_r / M_y	0.476	0.890	9.308	---

Stress values exceeding the yielding stress are nominal values.

Table 11 Comparison of Hydraulic Effect of Wave-head

Position	Nuckle Part	Roof at Lower End
Distance from Liq. Free Surface [mm]	410	577
Angle [degree]	47.0	27.4
Wave Velocity [cm/sec]		
i) From Value (A)	213	201
ii) From Value (B)	144	120
Impulsive Pressure by Testing [Kg/cm^2]	0.058	0.077
Estimated Impulsive Pressure [Kg/cm^2]		
i) Karman's Method from Value (A)	0.079	0.123
ii) Wagner's Method from Value (A)	0.108	0.221
iii) Karman's Method from Value (B)	0.035	0.045
iv) Wagner's Method from Value (B)	0.049	0.080
Tongue Shape Pressure by Testing [Kg/cm^2]	0.028	0.004
Estimated Tongue Shape Pressure [Kg/cm^2]		
i) From Value (A)	0.079	0.062
ii) From Value (B)	0.045	0.029

Wave Height are estimated by the following ways:
Value (A); Calculated wave height without the restriction of the roof excited by 3-wave sinusoidal input of 3.0 Hz, 30 Gal.
Value (B); Estimated wave height from the input wave velocity V_0 of FCOS-2.
All results are those observed at the test of FCOS-2.

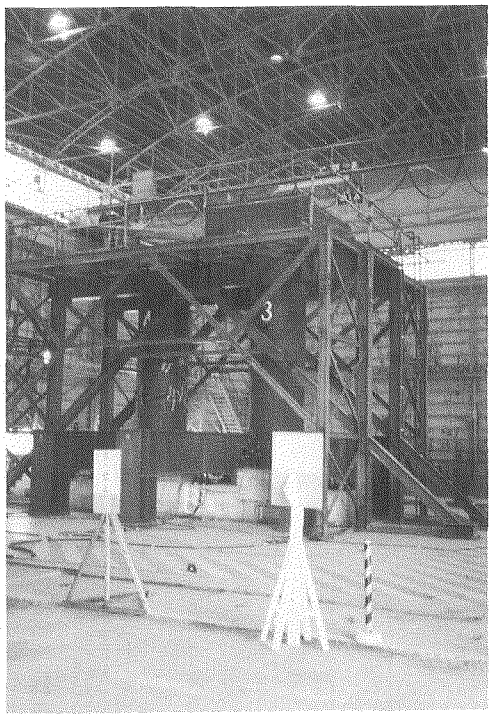

PICT. 1 TOWER MODEL (T-3) AND GUARD FRAME

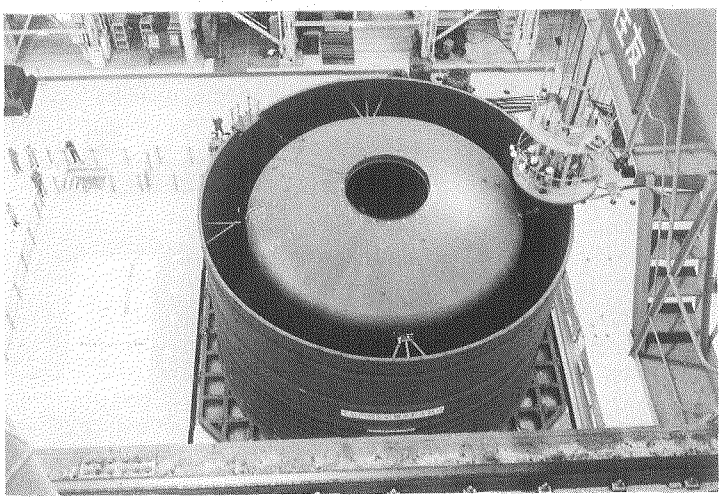

PICT. 2 TOP-VIEW OF INNER VESSEL
(THIN WALL STORAGE TANK) AND OUTER GUARD VESSEL

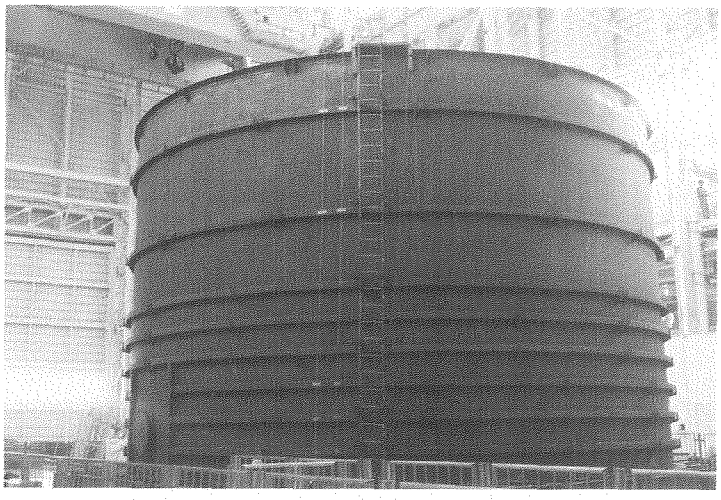

PICT. 3 OUTER GUARD VESSEL

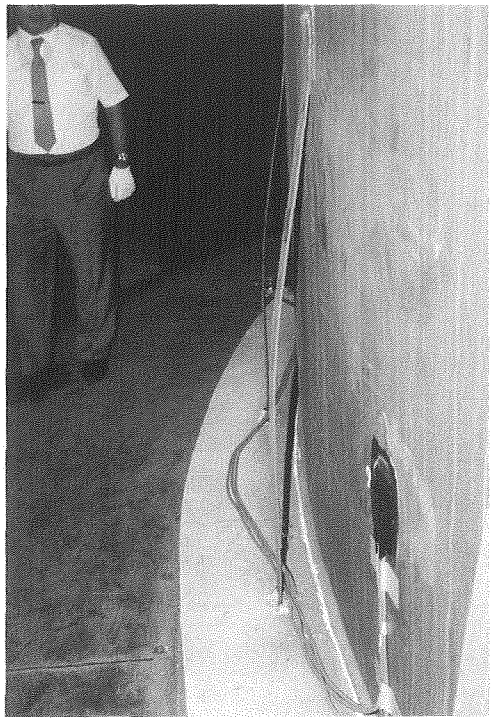

PICT. 4 LOSEN ANCHOR STRAPS

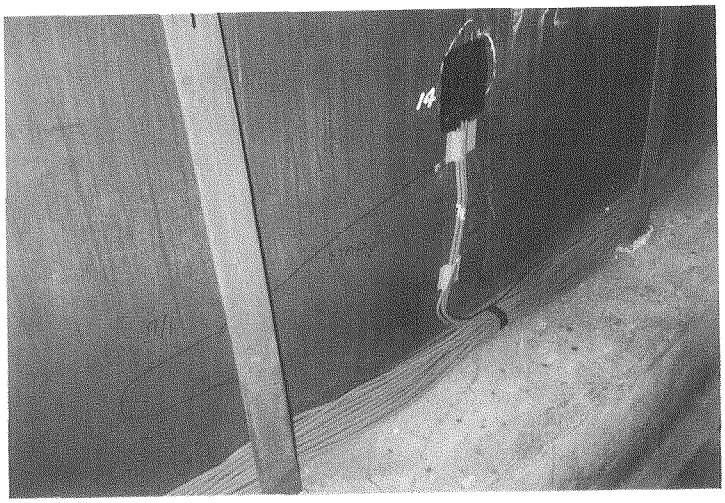

PICT. 5 BULGED PORTION OF CYLINDRICAL WALL

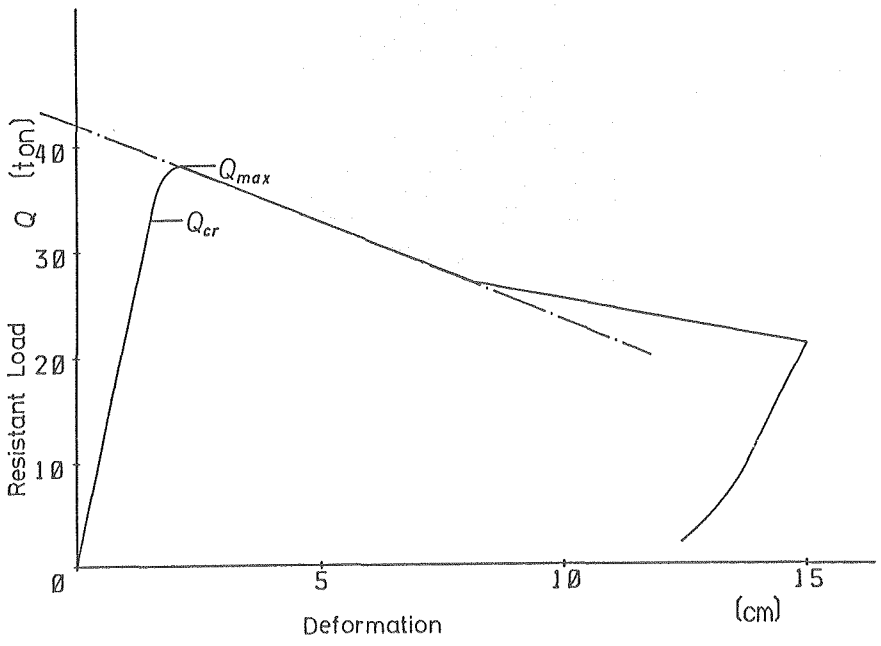

FIG. 1 STATIC DEFORMATION TEST OF TOWER MODEL T-1

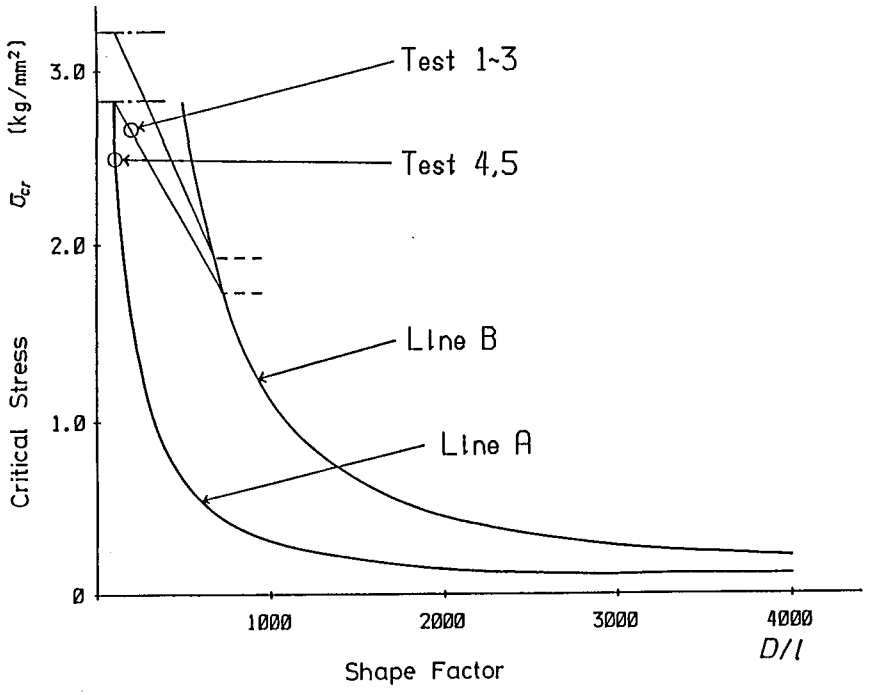

FIG. 2 THE RELATION OF CRITICAL STRESS σ_{cr} TO DIAMETER INDEX D/l OF TOWER MODEL

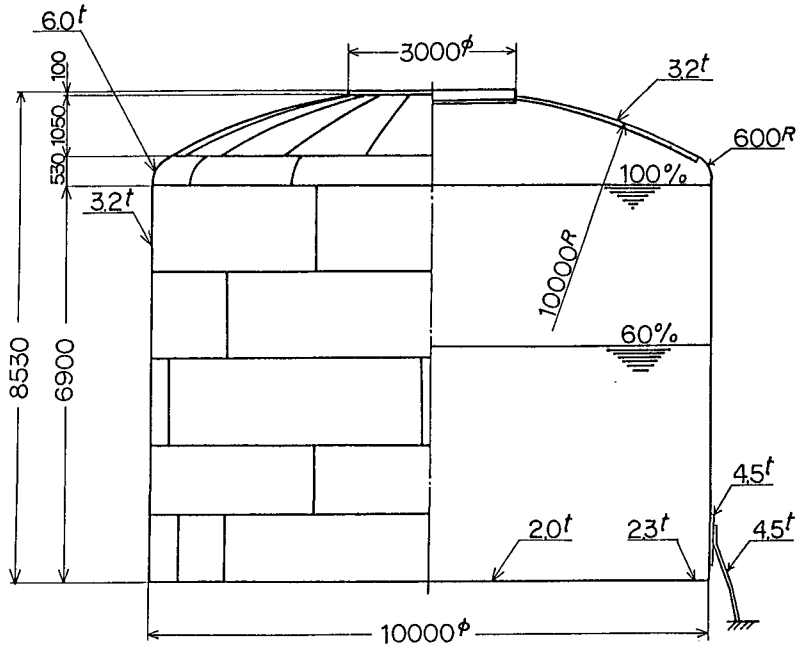

FIG. 3 SCHEMATIC DRAWING OF 500 TON THIN WALL TANK

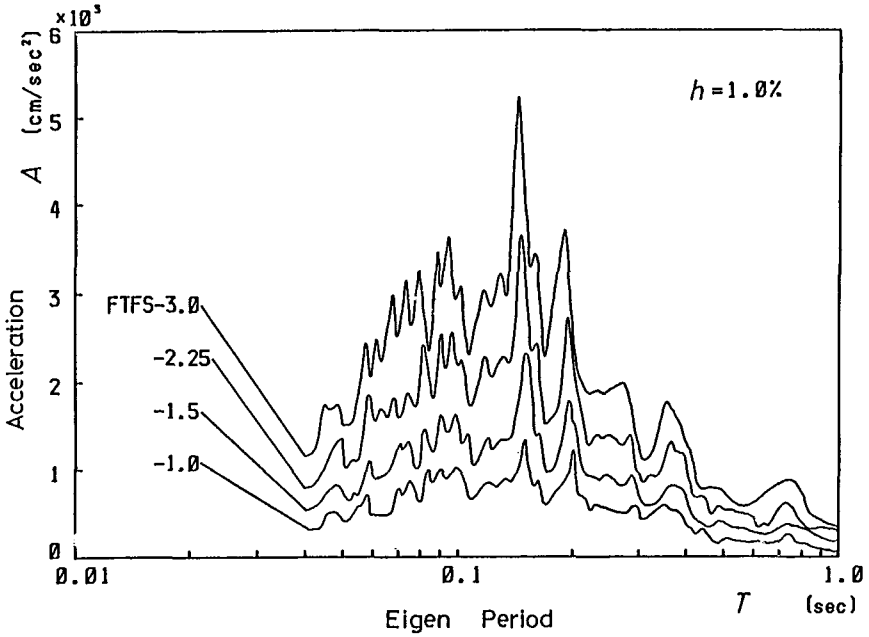

FIG. 4 RESPONSE SPECTRUM OF HORIZONTAL INPUT MOTIONS AT THE TABLE

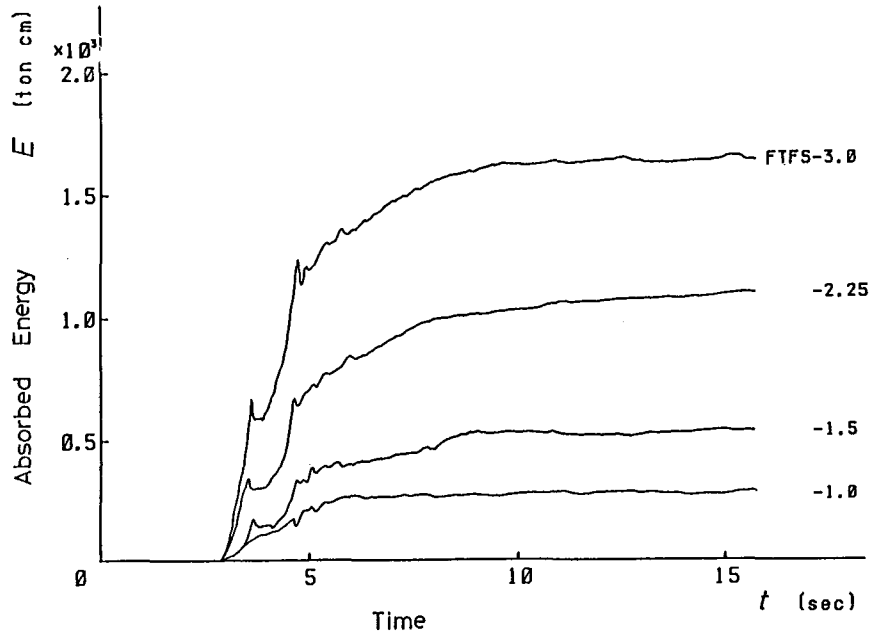

FIG. 5(A) TIME HISTORY OF ENERGY INPUT OF HORIZONTAL INPUT MOTIONS OBTAINED BY ACTUATOR REACTION FORCE

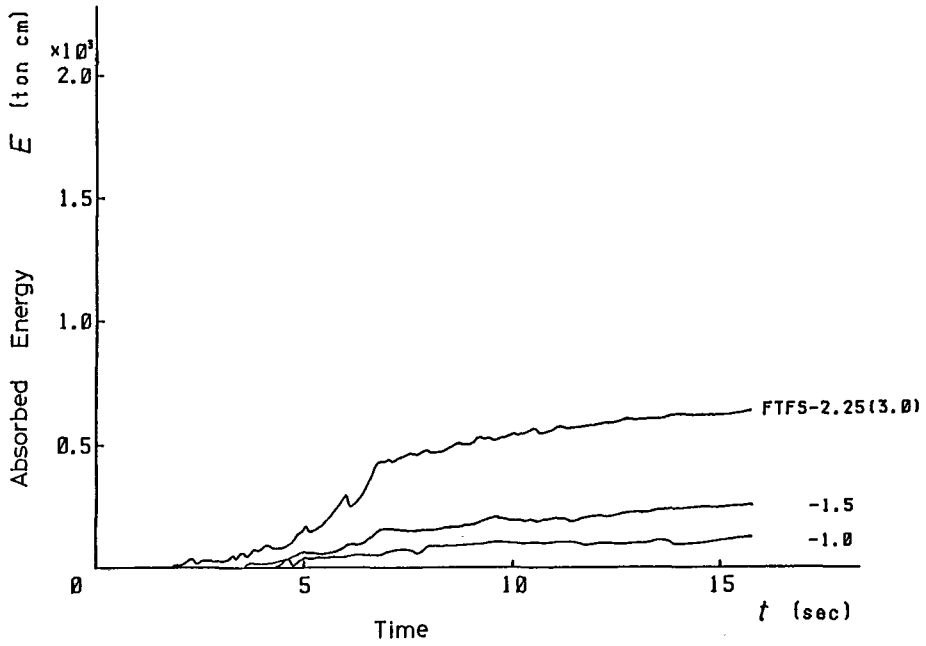

FIG. 5(B) TIME HISTORY OF ENERGY INPUT OF VERTICAL INPUT MOTIONS OBTAINED BY ACTUATOR REACTION FORCE

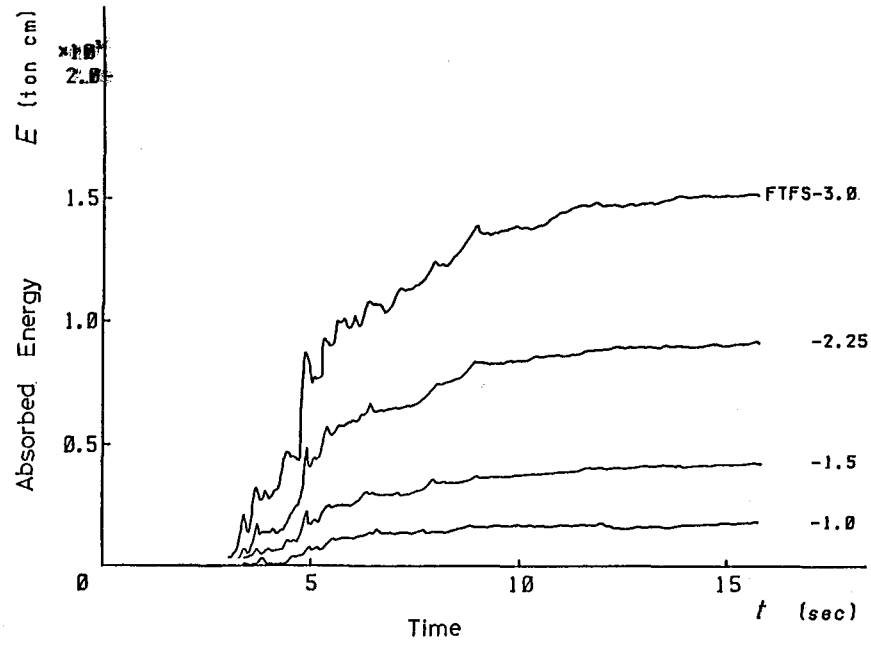

FIG. 6 TIME HISTORY OF ENERGY INPUT OF HORIZONTAL INPUT MOTIONS OBTAINED BY HYDRAULIC PRESSURE RESPONSE

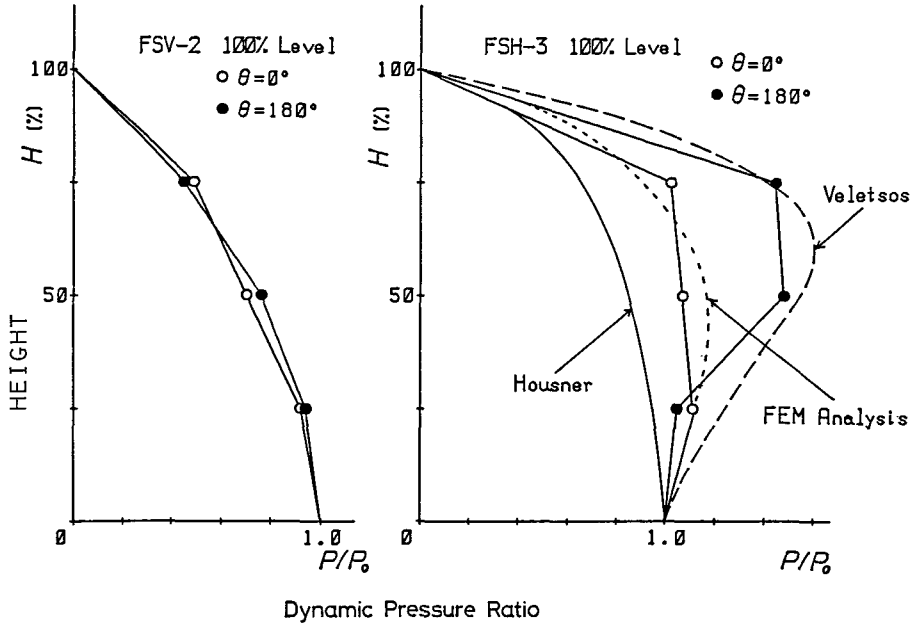

FIG. 7(B) DYNAMICS HYDRAULIC PRESSURE RESPONSE MODE BY VERTICAL EXCITATION

FIG. 7(A). DYNAMIC HYDRAULIC PRESSURE RESPONSE MODE BY HORIZONTAL EXCITATION

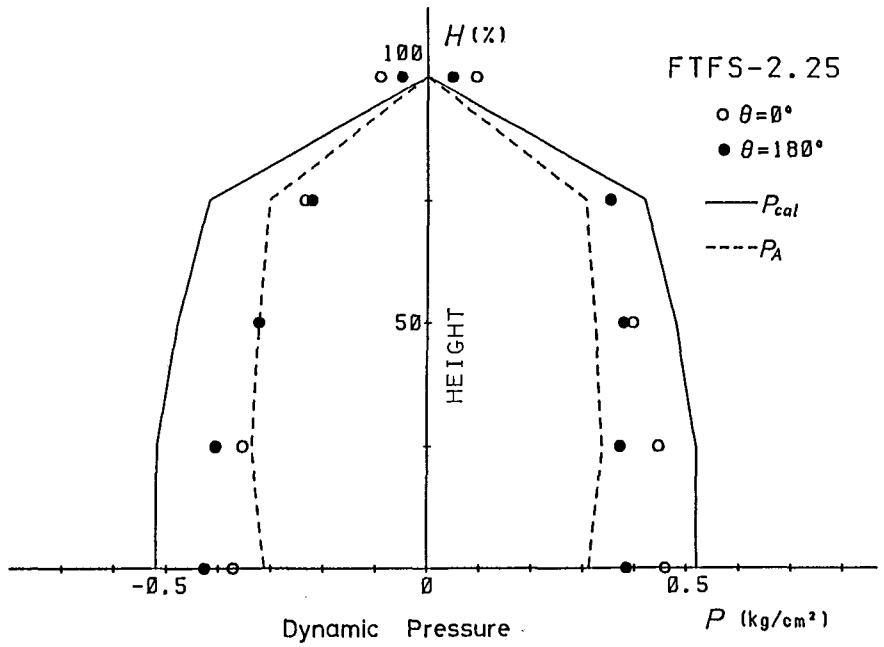

FIG. 8 COMPARISON OF TWO TYPES OF CALCULATED RESULTS P_{cal} AND P_A TO TESTING RESULTS OF DYNAMIC HYDRAULIC PRESSURE RESPONSE

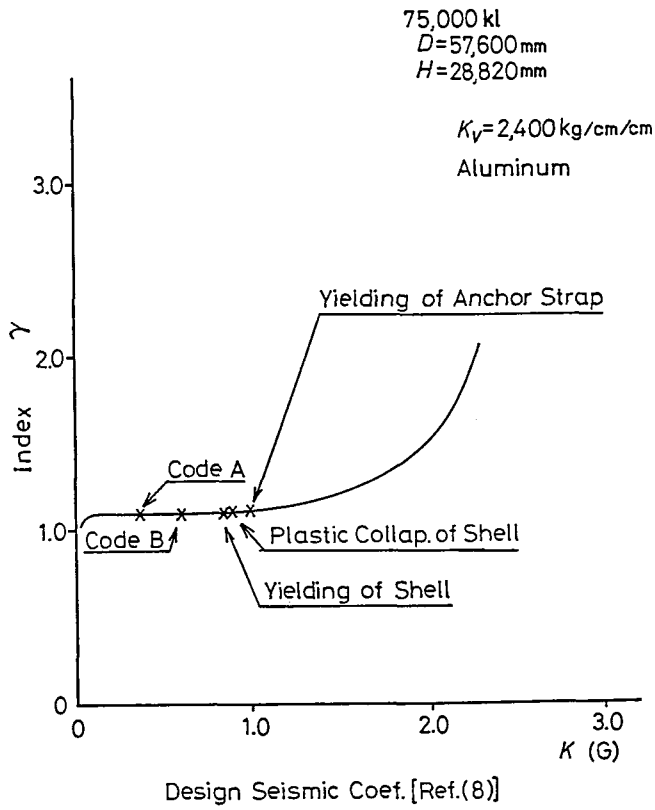

FIG. 9 STRESS INDEX FOR BENDING AT THE FOOT OF CYLINDRICAL WALL

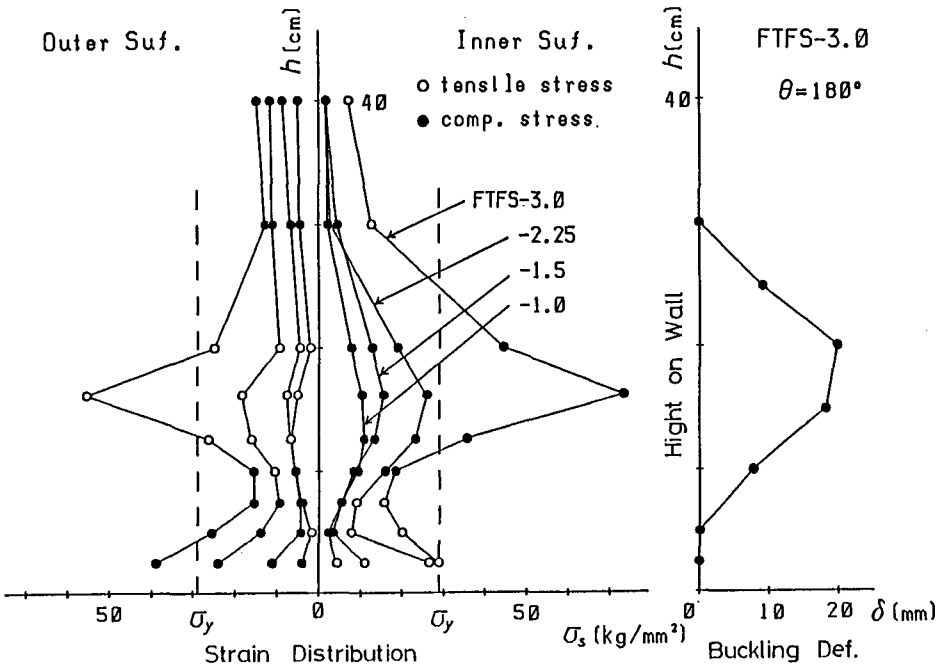

FIG. 10 MODE SHAPES IN NOMINAL STRAIN OF SHELL AND BULGING DEFORMATION

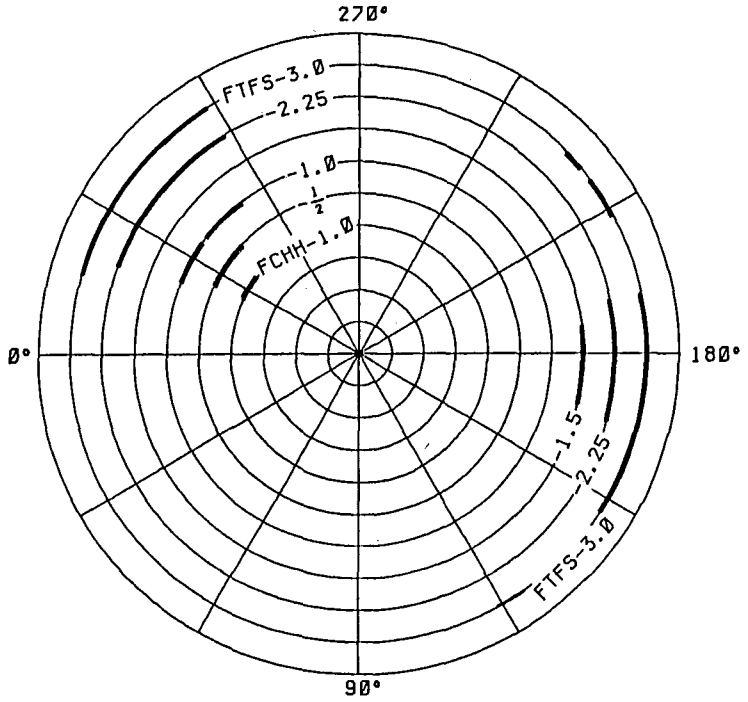

FIG. 11 DISTRIBUTION OF BULGED PARTS OF SHELL

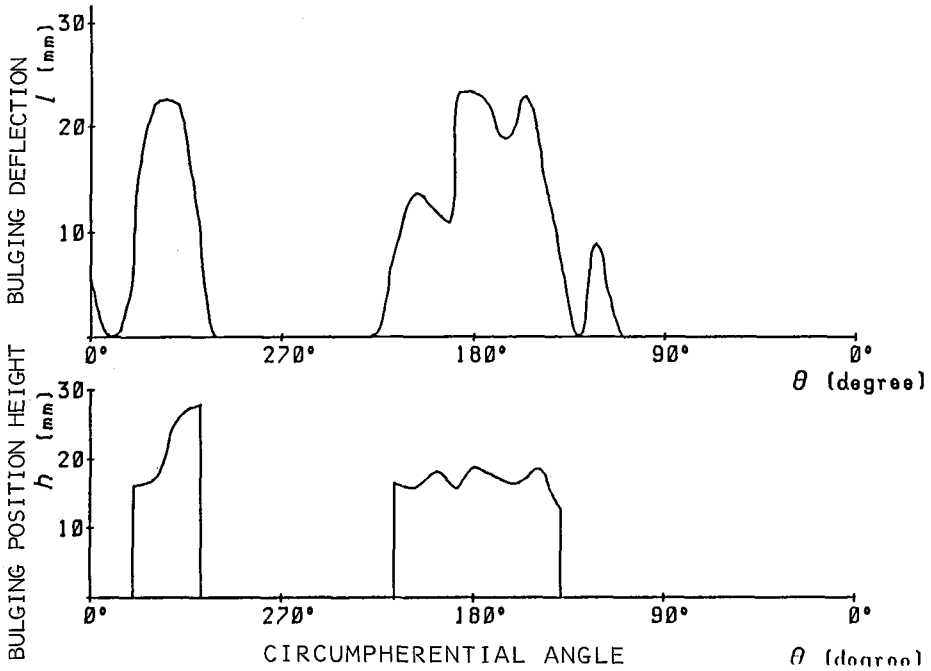

FIG. 12 DISTRIBUTION OF BULGING DEFORMATION OF SHELL AND THEIR POSITION IN WALL HEIGHT

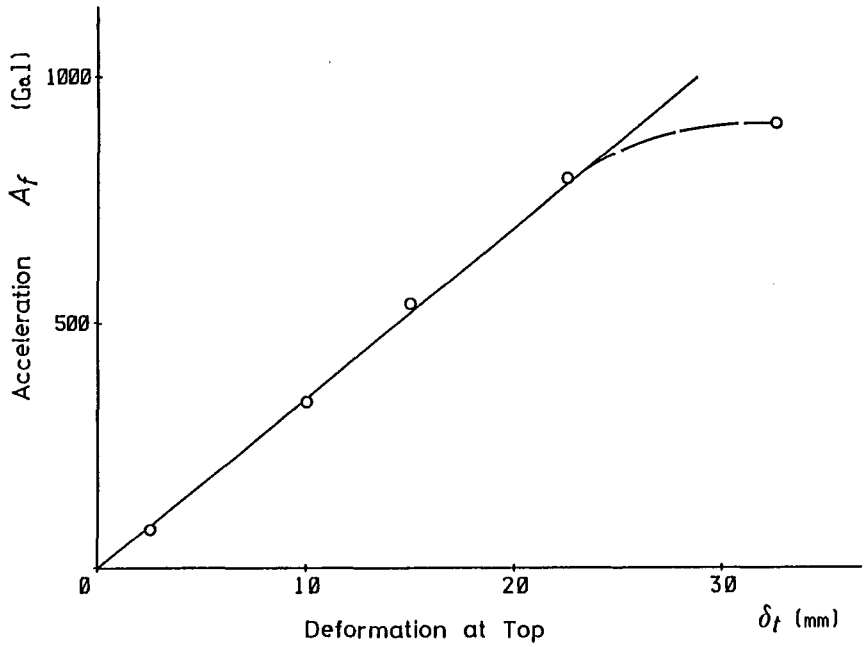

FIG. 13 DEFORMATION AT THE TOP OF SHELL

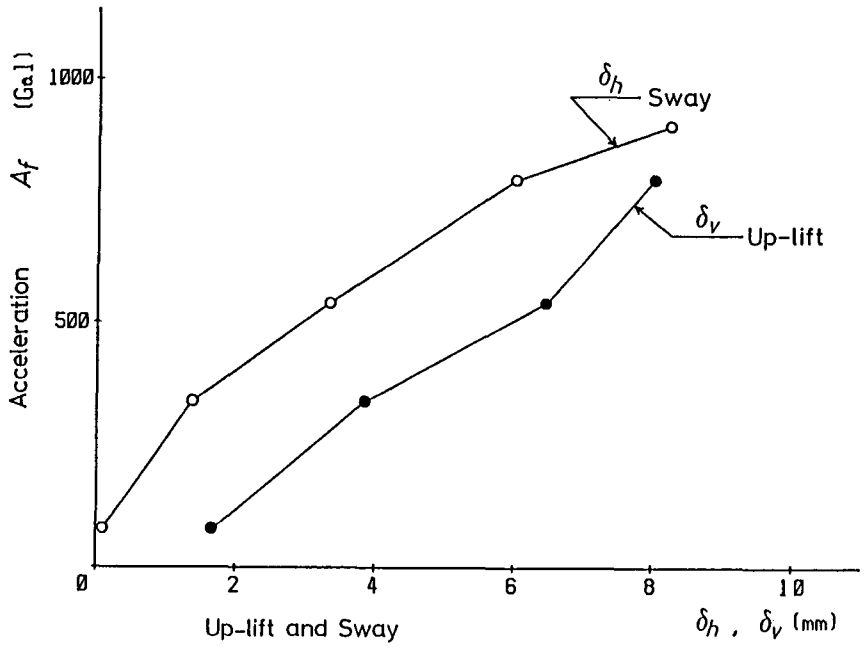

FIG. 14 SWAY AND UP-LIFTING AT THE BOTTOM OF SHELL

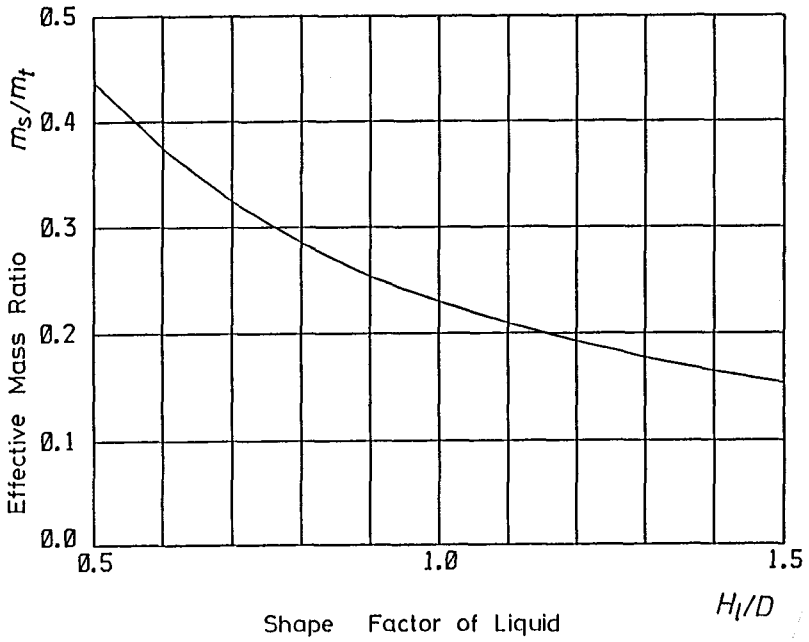

FIG. 15 EFFECTIVE MASS RATIO OF LIQUID TO ITS DEPTH (HEIGHT)